# Experimental dynamic analysis of the arch road bridge



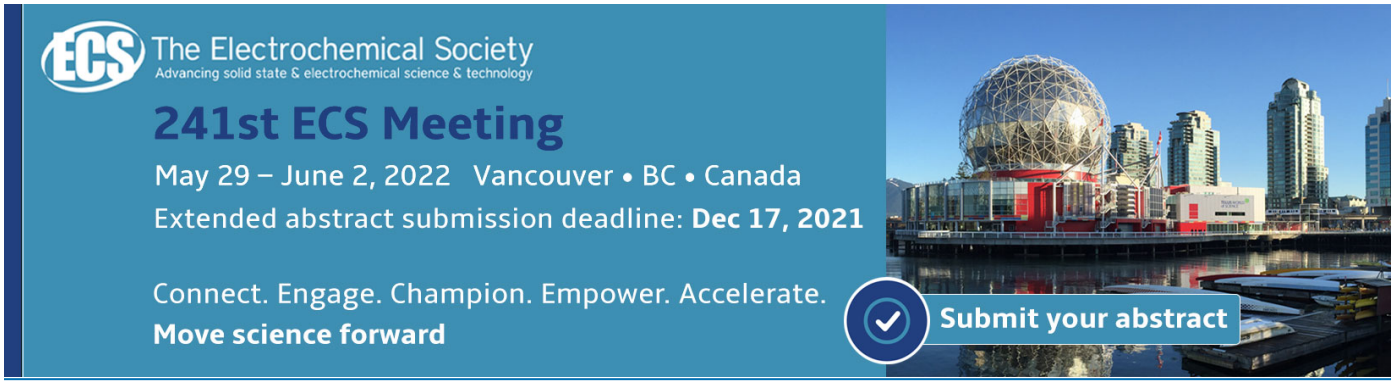

# Experimental dynamic analysis of the arch road bridge

**Tomáš Plachý[1], Michal Polák[1], Pavel Ryjáček[1], Milan Talich[2], Jan Havrlant[2], Filip Antoš[2], Jiří Litoš[1], Martin Macho[1], Lubomír Soukup[2]**

[1]Czech Technical University in Prague, Faculty of Civil Engineering, Thákurova 7, Prague 6, 166 29, Czech Republic
[2]Institute of Information Theory and Automation of the Academy of Sciences of the Czech Republic, Pod Vodárenskou věží 4, Prague 9, 166 29, Czech Republic

plachy@fsv.cvut.cz

**Abstract**. The paper presents an experimental dynamic analysis of the existing road bridge across the Labe river at Valy village in the Czech Republic. The observed structure is a bridge with 6 spans 23.1 m, 31.5 m, 84.0 m, 31.5 m and 23.1 m long. The horizontal load-bearing structure is a composite structure with two main steel girders and a lower reinforced concrete deck. The load-bearing structure is reinforced in the main span by the arch, this structural system is also called the Langer beam. The experiment was realized in three stages. The first one was performed in May 2020 before its opening, the second stage of the described experiment was realized in August 2020 and the third one was carried out in April 2021. The main purpose of the first stage was to determine in detail the natural frequencies and mode shapes of the whole bridge horizontal load-bearing structure also including the arch. The electrodynamic shaker, that was located on the bridge deck in the quarter of the main bridge span, was used for excitation of the bridge vibration. The measured characteristics of the natural vibration were compared with the calculated ones. Based on this comparison, the theoretical bridge model was verified. Basic objective of the second experiment stage was to verify new approach to dynamic response measurement – radar interferometry realized by two synchronized radars. The vibrations of the bridge caused by the standard road traffic and also by pedestrians were observed concurrently by both radar interferometry and classical approach realized by high sensitive piezoelectric accelerometers. The experiment was focused on the main span of the bridge only and the levels of forced vibration were observed primarily. However, the fundamental natural frequencies were also evaluated. The third stage was carried out by classical approach only. Again, the bridge vibration caused by the usual road traffic and pedestrians were measured in the main bridge span only because this section of the bridge was the most dynamically sensitive. Again, the levels of forced vibration were observed and the fundamental natural frequencies were determined. The evaluated natural frequencies from all three experiment stages were consequently compared.

## 1. Introduction

The experimental dynamic analysis described in this paper was realized on the existing road bridge across the Labe River at Valy village in the Czech Republic that was put into operation in June 2020 (see figure 1).

**Figure 1.** The view on the third span of the bridge where the structure is reinforced by the arch.

**Figure 2.** The bottom view on the load bearing structure in the second and first span of the bridge.

The experiment was realized in three stages and each one had its own purpose. Verification of the reliability of the bridge load bearing structure before its opening was the main objective of the first stage that included examination of the static and dynamic function of the bridge structure and validation of the theoretical (FEM) model used in the design of the bridge. Especially, the natural frequencies and corresponding mode shapes of the whole bridge horizontal load-bearing structure also including the arch were determined in detail.

Basic objective of the second experiment stage that was realized in mid-August 2020 was to verify new approach to dynamic response measurement – radar interferometry realized by two synchronized radars. The vibrations of the bridge were observed concurrently by both radar interferometry and classical approach realized by high sensitive piezoelectric accelerometers. Among others, the fundamental natural frequencies were also evaluated.

The third stage was carried out just by classical approach, that was performed in a simplified form only. Besides others, the fundamental natural frequencies of the bridge were determined. The evaluated natural frequencies from all three experiment stages were consequently compared.

Analogous experimental dynamic analysis was formerly performed on the existing footbridge across the Berounka River in Dobřichovice town. The vibrations of the footbridge deck were observed also by both radar interferometry and classical approach realized by high sensitive piezoelectric accelerometers. The analysis results were published in the reference [1].

Previously, the authors carried out some similar studies focused on different bridge structures based on experimental data obtained using classical approach [2-5] or the ground-based radar interferometry (GBRI) with ground-based real aperture radar (GB-RAR) performed by one radar only [6, 7].

There are some other references, for examples [8-11], where their authors described bridge analyses used the experimental data obtained by application of the radar interferometry realized by one radar only.

## 2. Description of the observed bridge

The observed structure is the bridge with six spans 23.1 m, 31.5 m, 84.0 m, 31.5 m and 23.1 m long. The horizontal load-bearing structure is reinforced in the main span by the arch, this structural system is also called the Langer beam (see figure 1).

**Figure 3.** The view on the load bearing structure in the third span of the bridge.

The typical cross section of the horizontal load-bearing structure of the bridge is a composite structure that consists of two identical main steel I shaped girders and a lower reinforced concrete deck (see figure 2). The lost formwork made from ultra-high performance concrete (UHPC) was used for the deck concreting. The steel cross girders are coupled with the concrete deck using the coupling pins. The main girders have constant height 1.80 m and the width of their lower and upper flange is 600 mm. The middle part of the main girders on their both sides is covered by the 8 mm thick steel protective shroud (see figure 3). The concrete deck thickness including the lost formwork is 250 mm. The road width between crash barriers is 6.50 m. Bridge walkways are located on cantilevers outside the main girders and their width is 2.50 m (see figure 3). The total width of the whole bridge cross section is 13.90 m.

The dimensions 600 mm x 600 mm of the welded square box cross section of the arch are uniform along whole arch span except the short part in the connection to the girder on arch ends (see figure 3). The steel bar-type arch hangers (see figure 1 and 3) are made of S460. The main girders, cross girders and the arches are made of S355.

## 3. The first stage of the experiment

As was said above, the first stage of the experiment was focused on verification of the reliability of the bridge and its dynamic and also static function and on the validation of the theoretical (FEM) model before its commissioning. The aim of the dynamic experimental analysis was to find out the real natural frequencies and modes of vibration of the bridge structure and then compare them with theoretical ones (see table 1, figure 7 and figure 9). The first stage of the experiment was realized using the standard measuring equipment.

### *3.1. Used standard measuring equipment*

In the course of the first experiment stage the bridge vibration was measured by eight piezoelectric acceleration transducers Brüel & Kjær Type 8344 (see figure 4). The working range of these sensors is from 0.2 Hz to 3 kHz. These transducers are very suitable for the dynamic experiments realized on bridges because the lower frequency limit of their working frequency range is low enough and they have very high sensitivity of approximately 2500 mV/g.

The sensors were via cables connected to the 8-channel data acquisition station SIRIUS Type 6ACC-2ACC+ made by DEWESoft. All channels have their own 2 × 24-bit A/D converter (so called DualCore) that is able to measure with dynamic range up to 160 dB. All A/D converter are mutually synchronized due to ensuring simultaneous measurement on all active channels.

**Figure 4.** The view on the three accelerometers of type 8344 placed on the main girder and on the roadway.

### *3.2. Used measurement system*

The electrodynamic shaker TIRAVIB 5140 was used for excitation of vibration of the observed bridge in the course of the first stage of the experiment. The shaker was situated on the deck eccentrically to the longitudinal axis of the bridge in the third quarter (section No. 16) of the main bridge span that is the 3rd one (see figure 5). The shaker position was selected as its best location on the deck based on the form of the first ten fundamental theoretical natural mode shape of vibration because of the most of them had some sufficiently high ordinate in this point to excite them. During the measurements, the vibration of the exciter weight was controlled to produce an excitation force of a random character.

The exciter control signal was designed such that the excitation force contained continuous frequencies ranging from about 0.3 to 20 Hz.

A grid of points (see figure 4, figure 7, figure 8 and figure 9 for example) was placed on the main girders, bridge deck and arch of the bridge to measure the response of the bridge. The position of the grid points was determined based on the character of the theoretical mode shapes (see figure 7 and figure 9 for example). The vibration was monitored in a total of 27 cross sections on the main girders and bridge deck and in 5 sections on the arches.

Two reference acceleration transducers were used in the experiment. The primary reference transducer measured the bridge vibration in the vertical direction and was located at point number 165 (the cross section No. 16), which was close to the exciter (see figure 5). The second reference transducer measured the vibration in the horizontal direction perpendicular to the longitudinal axis of the bridge and was located at point 125 (the cross section No. 12).

Five points were located in each monitored bridge deck cross section (see figure 4, figure 7, figure 8 and figure 9 for example). The vibration of the bridge deck and main girders was measured in the vertical direction at all grid points. In addition, at the edge points X5 of each section, the bridge vibration was measured in the horizontal direction perpendicular to the longitudinal axis of the bridge (see figure 4). In the sections on the arches, the vibration was measured in the vertical direction and on one arch in the horizontal direction perpendicular to the longitudinal axis of the bridge.

The response acceleration transducers were attached with neodymium magnets to steel weights, which were moved to the monitored points of the bridge deck (see figure 4). On the main girders, the transducers were attached directly to the steel girders using neodymium magnets (see figure 4).

### *3.3. Results of the first stage of the dynamic analysis*

In the preparation phase of the first stage of the experiment, the low damping of the analyzed road bridge was supposed because it is a steel composite structure. Thus, the Ambient Vibration Testing (AVT) system was chosen for the experimental modal analysis. The assumption about low damping of the bridge load bearing structure was indeed verified and it was fully confirmed as it is shown below.

If the AVT method is applied, the excitation forces induced by the shaker are not included to evaluation process and therefore the recorded dynamic responses of the bridge were normalized to the one measured in the reference point. Two reference responses were used during realization of the first stage of the experiment and also during evaluation of its results. The primary one was orientated in vertical direction in the third quarter of the bridge main span (the point No. 165) and the secondary one in the horizontal direction perpendicular to the longitudinal axis of the bridge in first quarter of the bridge main span (the point No. 125).

Measured records of the bridge vibrations were processed in software ME'scopeVES. At first, the measured data from all active channels were transformed using Fast Fourier Transform (FFT) from time domain to the frequency domain. Frequency transfer functions of the operational deflection shapes (ODS FRF) were evaluated from these signals for all 135 measured points on the bridge deck and 10 observed points on the arches.

The natural frequencies were evaluated from Complex Mode Indicator Function (CMIF), which is defined as the eigen values solved from the normal matrix, which is formed from frequency response function (FRF) matrix. CMIF can be computed from multiplication of normal matrix with its Hermitian matrix or by singular value decomposition (SVD) of normal matrix at each spectral line [12], [13]. The first ten natural frequencies (see table 1 and figure 6) and corresponding mode shapes

(for some examples, see figure 7, figure 8 and figure 9) were evaluated. They were compared with the appropriate theoretical natural frequencies (see table 1) and mode shapes (for two examples, see figure 7 and figure 9). As can be seen from table 1, a very good agreement between the measured and theoretical natural frequencies was achieved. It means, the theoretical model of the bridge was suitable enough.

**Figure 5.** The view on the electrodynamic shaker TIRAVIB 5140 situated on the bridge deck.

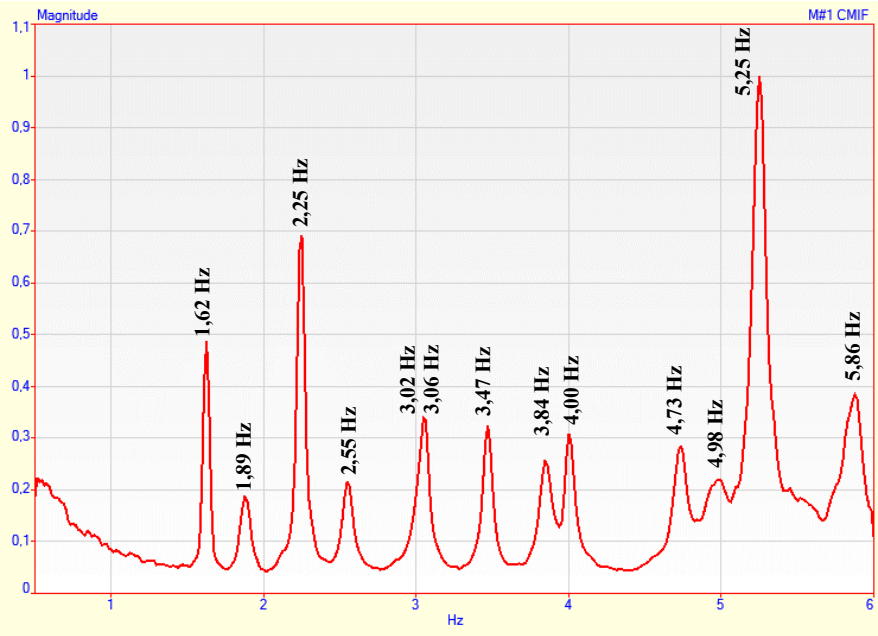


**Figure 6.** Evaluated Complex Mode Indicator Function (CMIF) with marked identified natural frequencies of the observed bridge.

The load bearing structure of the observed bridge that is designed for standard road traffic is unusually sensitive to the dynamic effects of the pedestrians. In particular, the main span of the bridge can noticeably vibrate when the pace frequency of walking pedestrians is close to the third natural frequency. The dynamic effect of the group of nine vandals was verified in the course of the first stage of the experiment. The peak value of vertical acceleration achieved 1.39 $m \cdot s^{-2}$ (see figure 10). The

corresponding RMS value of acceleration was 0.97 $m \cdot s^{-2}$. The measured acceleration was double integrated in the time domain using Simpson's rule, then the peak value of evaluated vertical deflections achieved 7.1 mm and RMS value of deflection was 5.0 mm.

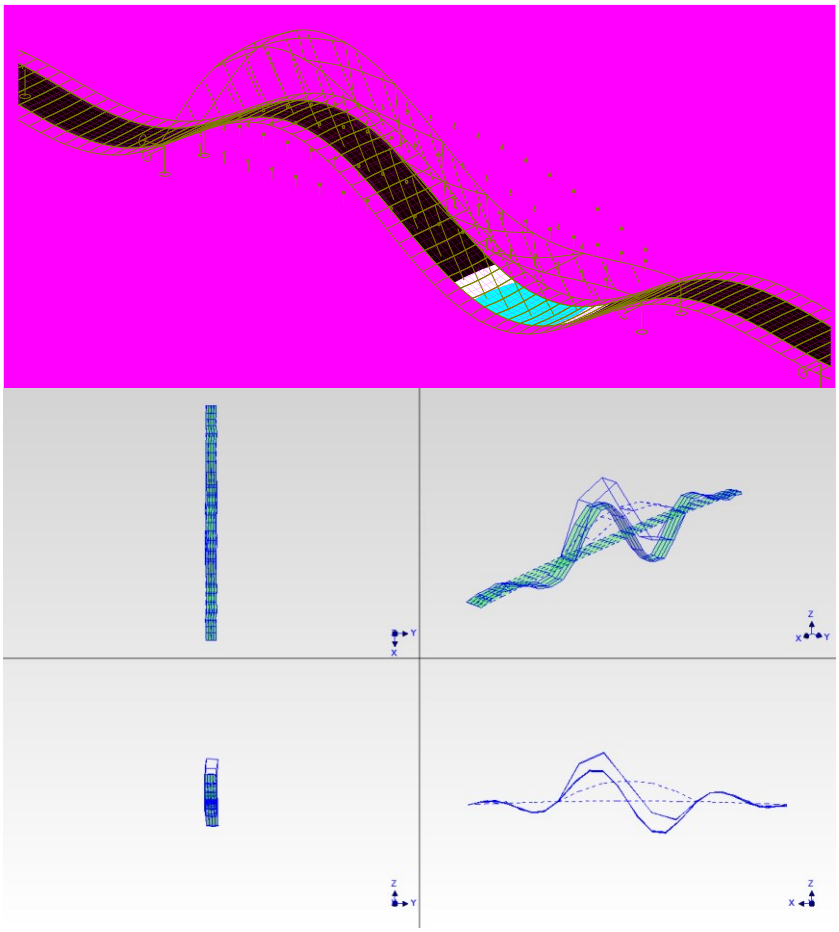

**Figure 7.** The visual comparison of the 1st theoretical natural mode (above) and 1st measured natural modes of vibration (bellow).

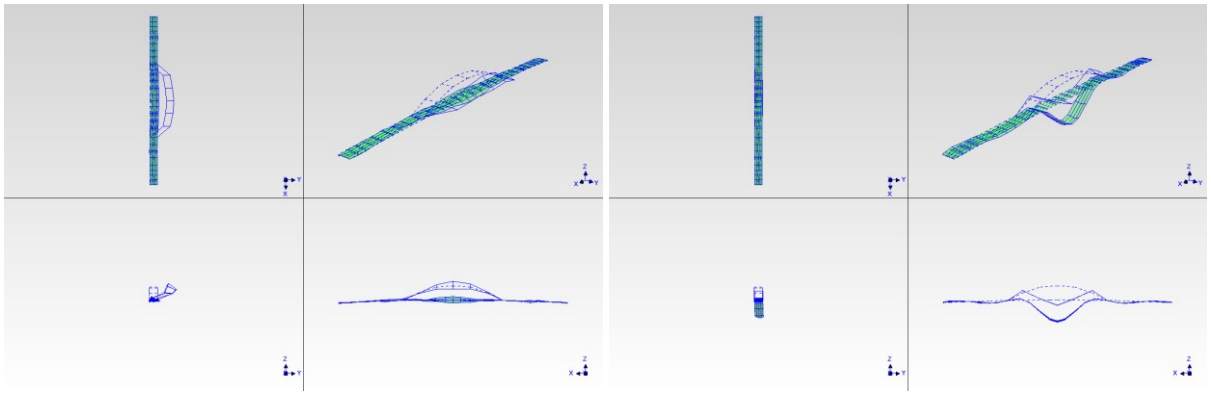

**Figure 8.** The measured 2nd (on left) and 3rd (on right) natural modes of vibration.

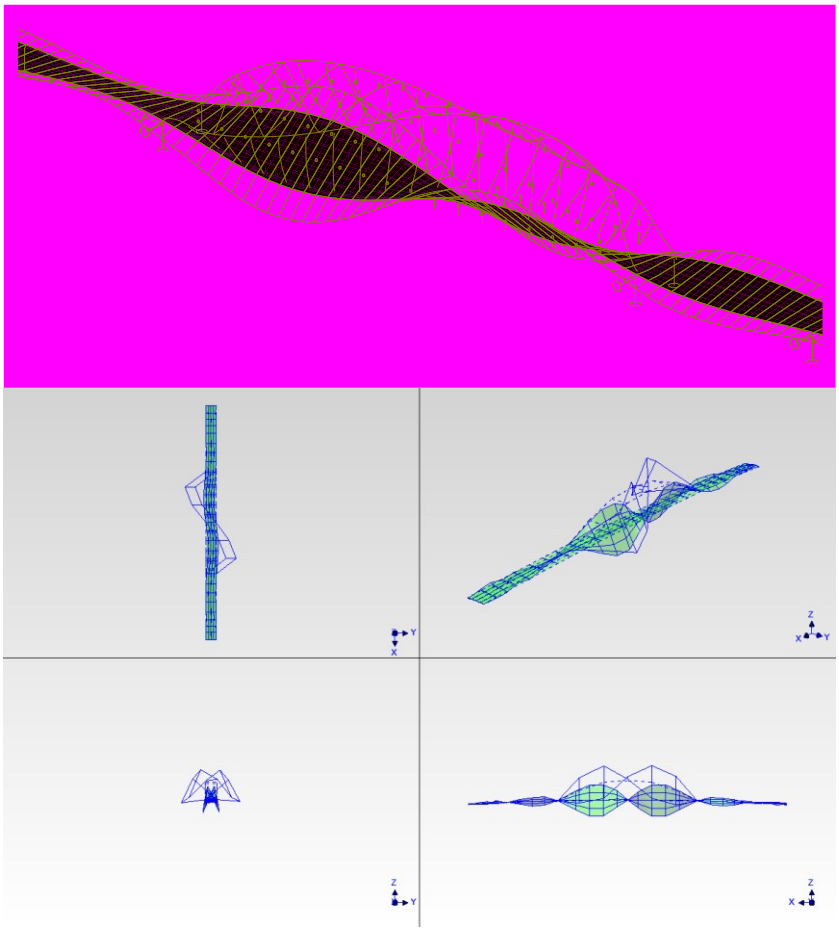

**Figure 9.** The visual comparison of the 4th theoretical natural mode (above) and 4th measured natural modes of vibration (bellow).

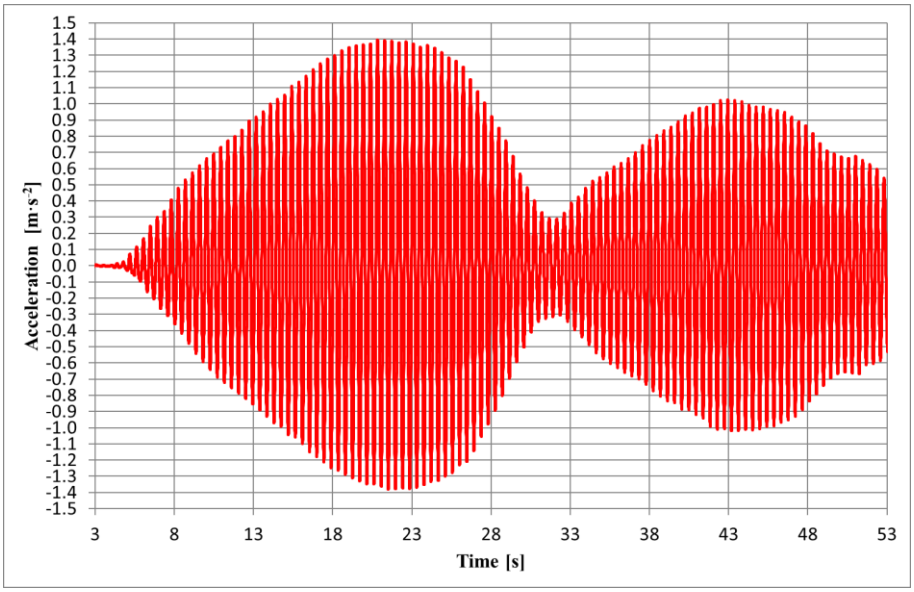


**Figure 10.** The record of the bridge vibration focused on vandalism at the natural frequency $f_{(3)}$ = 2.25 Hz.

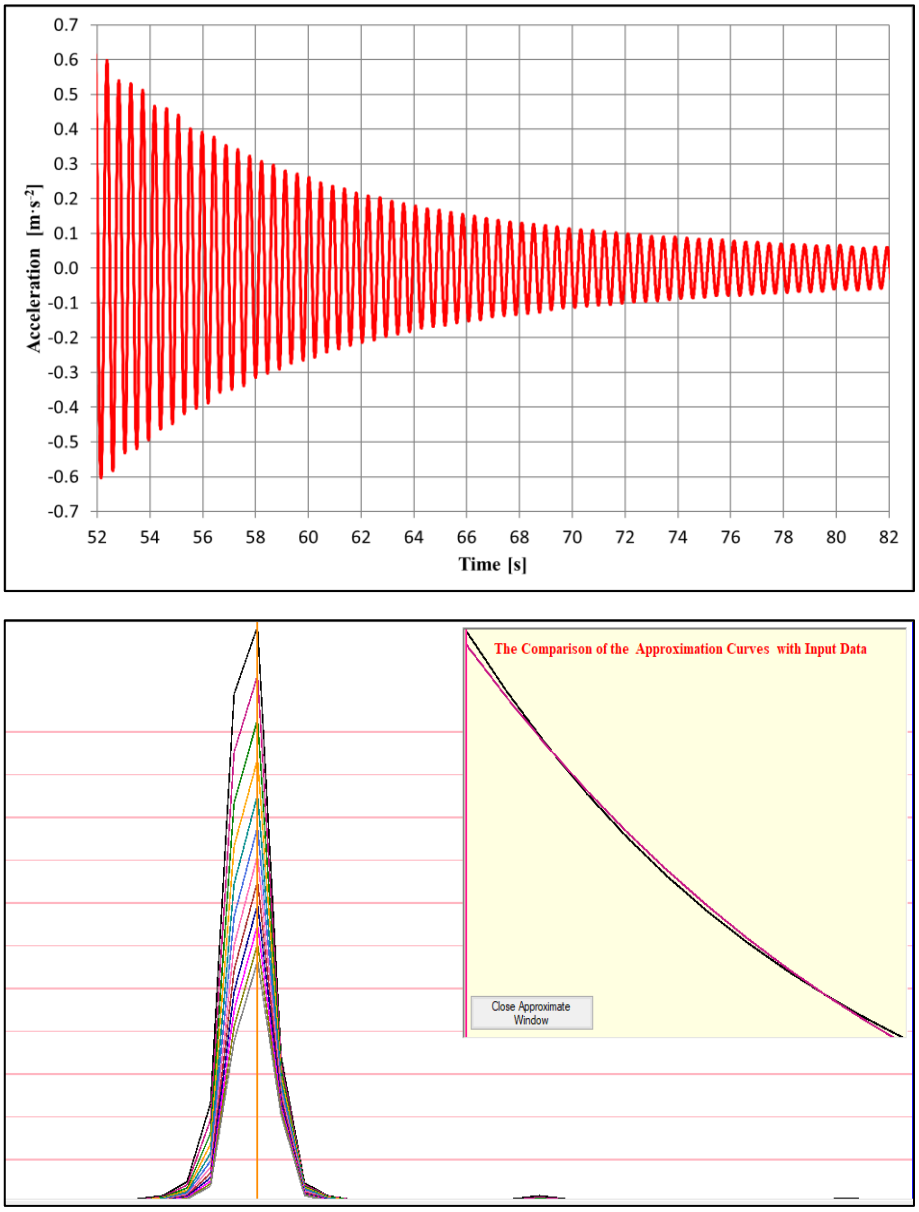


**Figure 11.** The damping evaluation from the record of the bridge vibration focused on vandalism at the natural frequency $f_{(3)}$ = 2.25 Hz (corresponding logarithmic decrement $\delta_{(3)}$ = 0.035), the processed time course of acceleration (above) and evaluated FFT multispectrum (below).

The logarithmic decrement δ of the bridge damping was evaluated from suitable records of the bridge dynamic response for the fundamental natural frequencies. A significant level of free vibration at the end of the record in which the dynamic effects of a group of vandals were observed was used for this purpose (see figure 11). The damping was evaluated using FFT multispectrum. One example of that approach for the natural frequency 2.25 Hz is shown in figure 11 where the window with comparison of the evaluated data by FFT multispectrum (the black curve) with the theoretical exponential approximation function calculated using root mean square method (the violet curve) is also included.

For example, the logarithmic decrement $\delta_{(1)}$ = 0.025 ±0.003 was evaluated for the natural frequency $f_{(1)}$ = 1.62 Hz, the logarithmic decrement $\delta_{(3)}$ = 0.035 ±0.003 for the natural frequency $f_{(3)}$ = 2.25 Hz

(see figure 11), the logarithmic decrement $\delta_{(4)} = 0.067 \pm 0.005$ for the natural frequency $f_{(4)} = 2.25$ Hz and the logarithmic decrement $\delta_{(5)} = 0.066 \pm 0.005$ for the natural frequency $f_{(5)} = 3.02$ Hz.

**Table 1.** Natural frequencies of the observed bridge evaluated during the first stage of the experiment and their comparison with the corresponding theoretical ones.

| No. (j) | Measured f(j) [Hz] | Corresponding theoretical f(j) [Hz] | Difference between frequencies [%] | Character of the natural mode |
|---|---|---|---|---|
| **(1)** | 1.62 ± 0.02[a] | 1.55 | -4.7 ± 1.3[a] | 1st vertical bending mode of vibration |
| **(2)** | 1.89 ± 0.02 | 1.90 | +0.7 ± 1.1 | 1st horizontal mode of vibration of arch |
| **(3)** | 2.25 ± 0.02 | 2.22 | -1.4 ± 0.9 | 2nd vertical bending mode of vibration |
| **(4)** | 2.55 ± 0.02 | 2.43 | -4.9 ± 0.8 | 1st torsional mode of vibration |
| **(5)** | 3.02 ± 0.03 | 3.03 | +0.3 ± 1.0 | 2nd torsional mode of vibration |
| **(6)** | 3.06 ± 0.03 | 3.19 | +4.1 ± 0.9 | 3rd vertical bending mode of vibration |
| **(7)** | 3.47 ± 0.02 | 3.44 | -0.8 ± 0.6 | 4th vertical bending mode of vibration |
| **(8)** | 3.84 ± 0.02 | 3.88 | -3.1 ± 0.5 | 3rd torsional mode of vibration |
| **(9)** | 4.00 ± 0.02 | 3.90 | +1.5 ± 0.5 | 5th vertical bending mode of vibration |
| **(10)** | 4.73 ± 0.02 | 4.55 | -3.9 ± 0.4 | 4th torsional mode of vibration |

[a] Expanded uncertainty $U_{k=2}$.

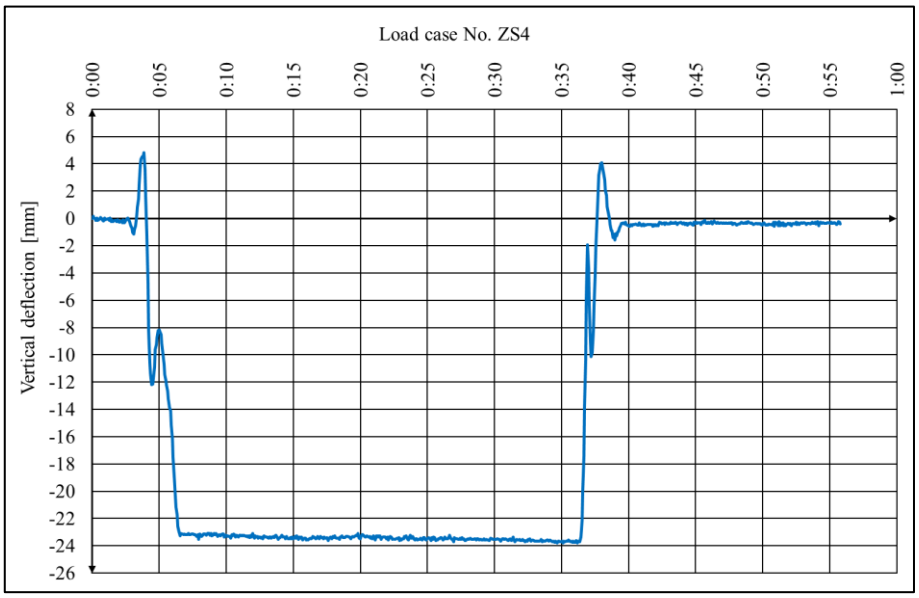


**Figure 12.** The time record of the vertical deflection of the right main girder in third quarter of the main bridge span.

The technique called Digital Image Correlation (DIC) was also applied during the first stage of the experiment but it was used in the course of the static load test only. Vertical deflection of the bridge main span in its third quarter that is drawn in figure 12 was measured by this technique. The obtained results were substantially more stable than ones measured using geodetic leveling and it was noticeable especially for the load case No. ZS4 (see figure 12).

## 4. The second stage of the experiment

The second stage of the experiment was realized on 13th August 2020 in a simplified form compared to the first stage. The first objective was to observe and evaluate the levels of forced vibrations caused

by the standard road traffic and pedestrians. The second one was to compare them with results simultaneously measured by radar interferometry. The last one was to determine the fundamental natural frequencies of the bridge and to compare them with frequencies obtained in the first stage.

*4.1. Used standard measuring equipment and corresponding measurement system*

The standard measuring equipment used in the second stage was similar to the one applied in the first stage but the acceleration transducers were placed in the same positions during the whole measurement because it was focused on forced vibration. The transducers were placed in the points No. 111, 121, 141, 161 on the left main girder. The response was measured in vertical direction in all points and in horizontal direction perpendicular to the longitudinal axis of the bridge in all points except the No. 111.

The standard road traffic was not limited during the second experiment stage. It means, that the bridge vibrations measured in the course of the bridge observation were induced only by vehicle passages over the bridge deck and by movement of pedestrian groups over sidewalks. The pedestrians walk was synchronized generally. The step frequency was controlled by a metronome and it was selected to achieve resonance with some fundamental natural frequencies of the bridge deck.

*4.2. Used radar interferometry and corresponding measurement system*

As mentioned above, the basic goal of the second stage of the experiment was to verify a new technology for measuring the dynamic response using ground-based radar interferometry (GBRI) with ground-based real aperture radar (GB-RAR) performed by two synchronized radars. The GBRI method has the ability to measure real-time deflections at normal operating conditions with precision better than 0.1mm. Deflections of a monitored object can be simultaneously determined at multiple locations. So it is possible to obtain both general and detailed information on the behavior of the structure under its dynamic load. For example, on the bridge of a length of 100m is possible to simultaneously monitor up to about 100 points. In recent literature are the basic principles and examples of the use of GB-RAR technology for determining deflection of bridges given e.g. in [6], [7], [10] and [11].

During the measurements, climatic conditions were recorded using a data logger and a video recording of the traffic on the road on the bridge was taken. The local situation and position of the radars were mapped by detailed terrestrial laser scanning and subsequently a 3D model was processed.

The measurement was performed during normal road traffic on August 13, 2020 in the period from 10:00 am to 11:00 am simultaneously with the standard measuring equipment described in chapter 4.1. In addition, vibrations of the bridge were caused by several people during the measurements. Climatic conditions during the measurement: temperature 25.1°C - 26.3°C, humidity 55.4 – 51.0%, wind speed 0 - 1 m/s in a variable direction. Two Radars IBIS Italian manufacturer Ingegneria Dei Sistemi (IDS) were used for the measurements. Radar R1: IDS Radar IBIS – FS Plus, radar R2: IDS Radar IBIS – RU 172. In both cases, IBIS-ANT3-H17V15 antennas were used. See table 2 for more details on radar settings.

**Table 2.** Settings of used radars.

| | $R_1$: **IDS Radar IBIS – FS Plus** | $R_2$: **IDS Radar IBIS – RU 172** |
|---|---|---|
| **Sampling frequency** | 200 Hz | 199.2 Hz [a] |
| **Signal range (max. distance)** | 75 m | 70 m |
| **Rbin (range resolution area)** | 0.75 m | 0.75 m |

[a] The set value was 200 Hz, the actual value (corrected by the radar control software) was 199.2 Hz.

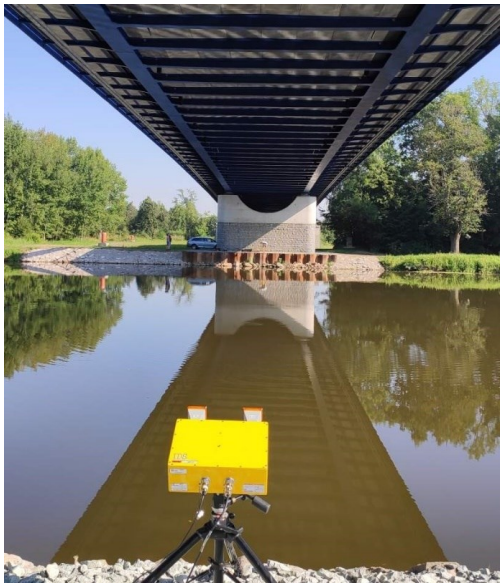

**Figure 13.** View of the steel crossbeams of the bridge from the position of the R2 radar (near Valy village). The crossbeams served as natural signal reflectors.

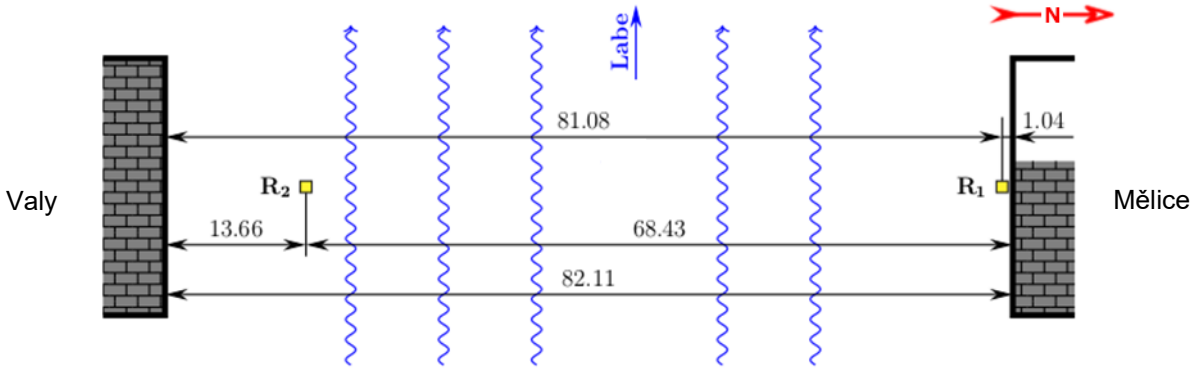


**Figure 14.** Top view of the location of radars under the third (main) span of the bridge.

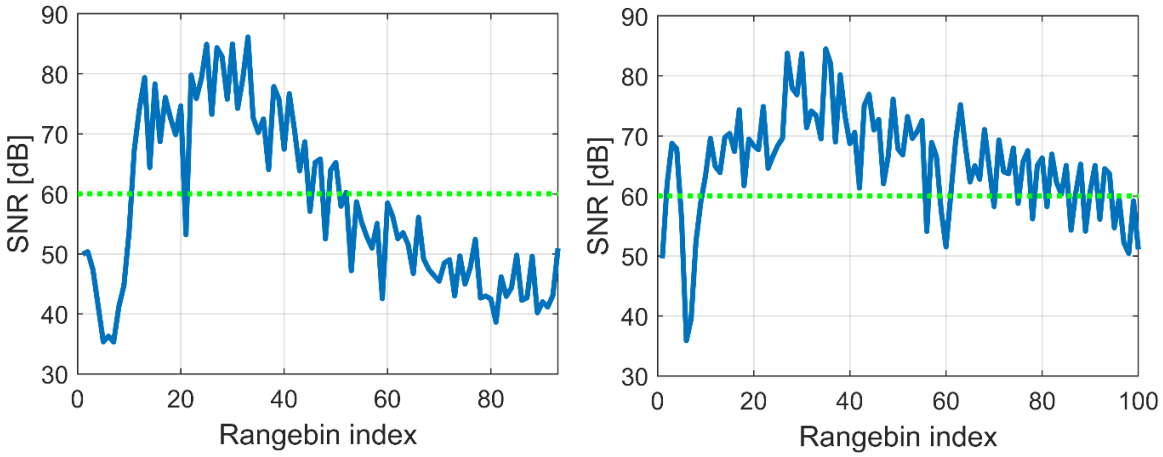


**Figure 15.** Significant maxims on the SNR profiles of the radars R1 (left) and R2 (right).

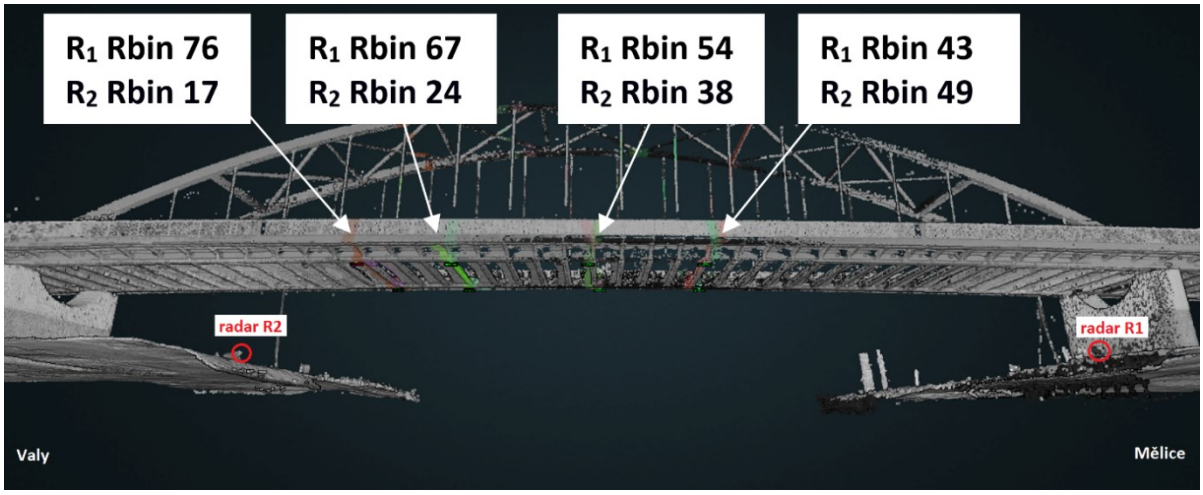


**Figure 16.** 3D model of the bridge with colour-highlighted Rbins for radars R1 and R2, which were evaluated.

**Figure 17.** Passage of the vehicle in the direction from Mělice to Valy (left) and back (right).

The dynamic measurement of the bridge was performed with two interferometric radars simultaneously. Radar R1 was located on the right bank of the river Labe (near the Mělice village) by the foot of the bridge support approximately in the axis of the bridge deck. The second radar R2 was located on the left bank (near the Valy village) closer to the river. The vertical tilt of both radars was determined experimentally so as to cover the maximum length of the main field and to avoid significant mutual interference of the radar signal. A view of the steel crossbeams of the bridge from the position of the R2 radar (near Valy village) is shown on figure 13. The crossbeams served as natural signal reflectors. A top view of the location of radars under the third (main) span of the bridge is shown on figure 14.

Significant maxims were selected on the range profiles (SNR profiles) of both radars (see figure 15), which correspond to the position of the steel crossbeams of the bridge structure. These selected maxims determine the selection of Rbins for evaluation. Only those Rbins that have sufficient signal strength on both radars were selected. Selected Rbins (crossbeams) are highlighted in figure 16.

*4.3. Results of the second stage of the dynamic analysis obtained by the radar interferometry*

Three cases occurring during the measurement were evaluated in more detail. The first case was the passage of a vehicle (a van) in the direction from Mělice to Valy (see figure 17). The second case was the passage of a vehicle (a van) in the opposite direction, i.e. from Valy to Mělice (see figure 17). The last case was the evaluation of the vibration of the bridge structure, which was caused by a group of several people walking at regular step.

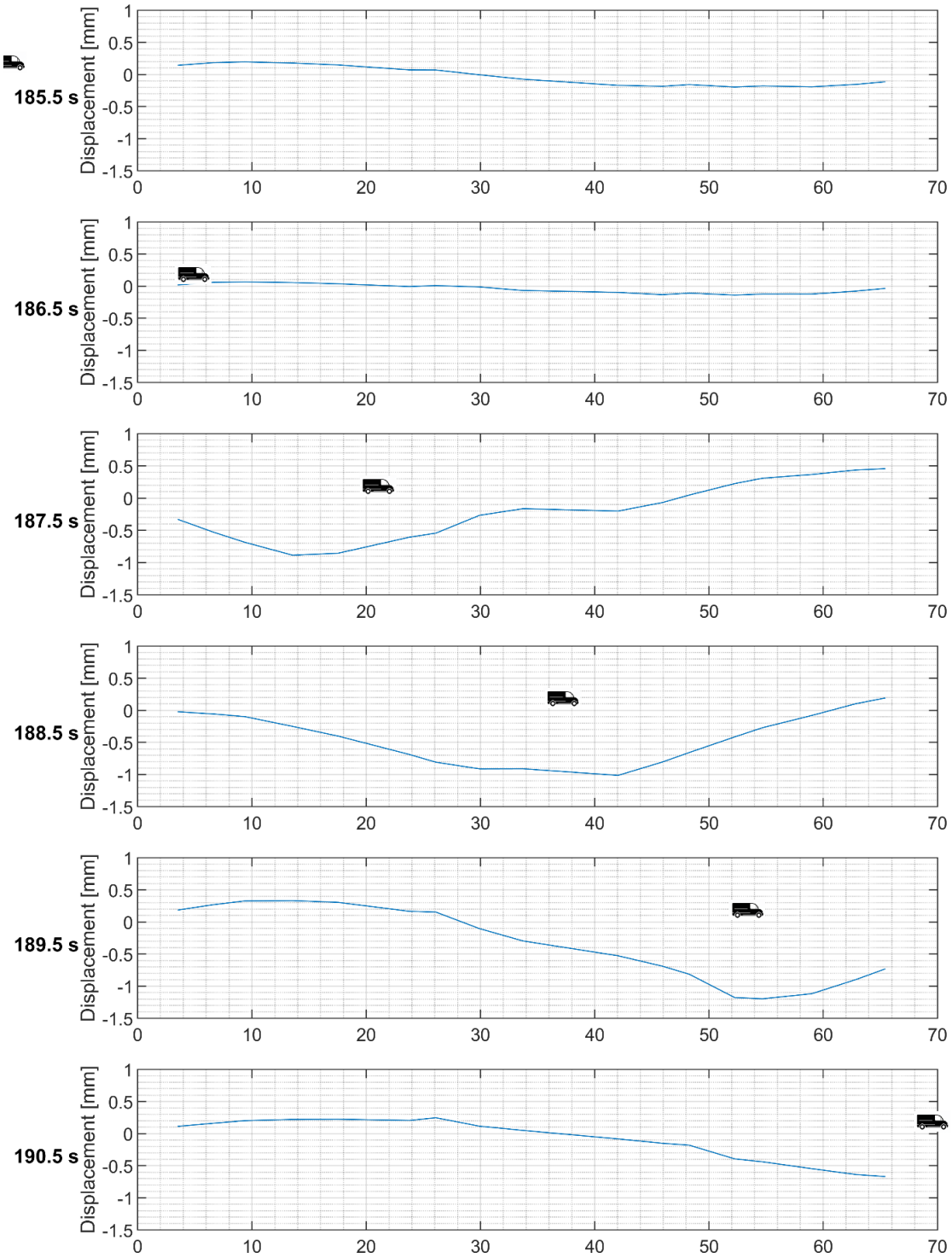


**Figure 18.** Graphic representation of the bridge deck vertical deflection of the entire third (main) span of the bridge during time when the vehicle (van) passes in the direction from Mělice to Valy.

The passage of the vehicle caused a vertical deflection of approx. 1.2 mm in the middle of the bridge, followed by a lift of approx. 0.5 mm. This value was determined by both radars. Also, the character of the development of deflections over time determined by both radars was approximately

the same. It is an independent control of measurements indicating the achievement of high accuracy in determining the size of deflections. The resulting vertical deflections caused by the passage of the vehicle are shown in figure 19.

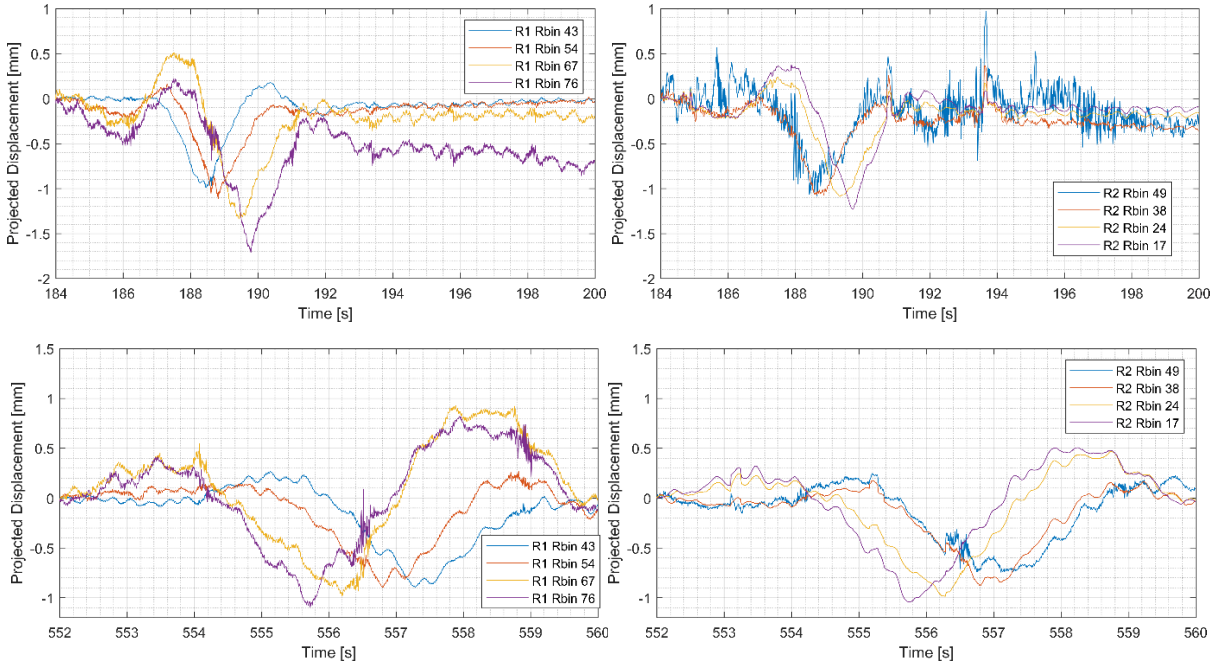


**Figure 19.** Vertical deflections measured by radar R1 (left) and R2 (right) on the identical four selected crossbeams (Rbins) during the passage of the vehicle in the direction from Mělice to Valy (above) and in the opposite direction (below).

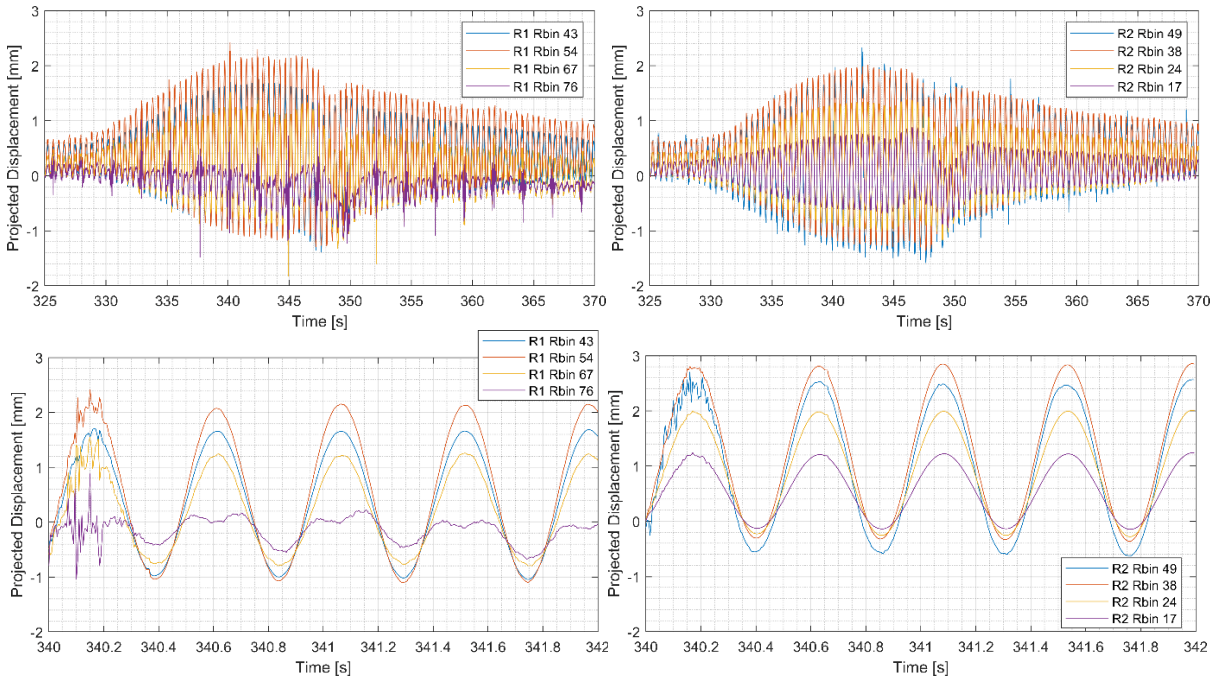


**Figure 20.** Vertical deflections, caused by several people, measured by radar R1 (left) and R2 (right) on the identical four selected crossbeams (Rbins), during 45s (above) and detail during 2s (below).

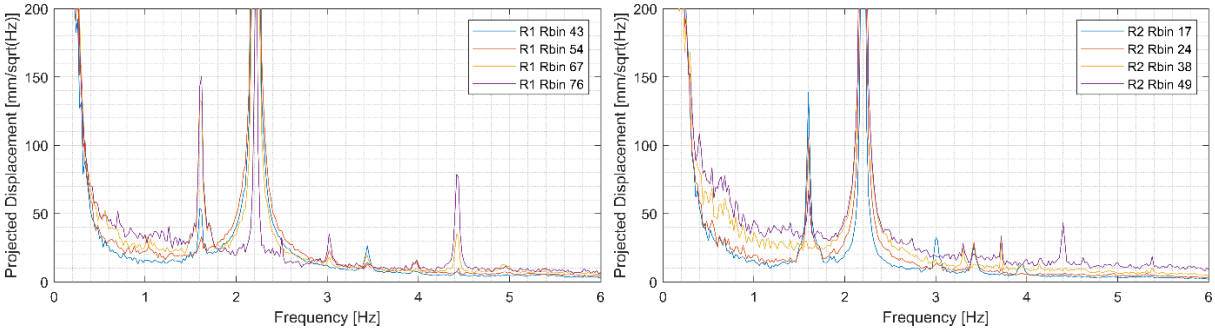


**Figure 21.** Periodograms – natural, significant and distinct frequencies of the observed bridge measured by radar R1: 1.62, 2.22, 3.02, 3.44, 4.42 Hz (left) and by radar R2: 1.60, 2.22, 3.02, 3.30, 3.42, 3.71, 4.40 Hz (right), on the selected crossbeams (Rbins).

The graphic representation of the bridge deck vertical deflection in the entire third (main) span of the bridge during time when the vehicle (the van) passes in the direction from Mělice to Valy is shown at figure 18. This is a simple visualization that shows the displacement of the maximum vertical deflection of the bridge deck together with the position of the passing vehicle. While under the passing vehicle there is a maximum deflection of about 1.2 mm, at the other end of the bridge deck there is a lift of about 0.5 mm at the same time.

The oscillation of the bridge deck, which was caused by the group of several people walking at regular step, caused vertical deflections with a maximum range of about 3.2 mm. Also in this case, both radars determined the same value of vertical deflections. The resulting vertical deflections caused by the regular step of several people are shown in figure 20.

To determine the natural frequencies of the observed bridge, a frequency analysis was performed using a discrete Fourier transform (DFT) - see e.g. [14]. The result of the analysis are the periodograms drawn in figure 21. The evaluated significant and distinct frequencies are stated in the description of the figure 21 and some selected ones are mentioned in table 3.

*4.4. Results of the second stage of the dynamic analysis obtained by the classical approach*

In the second stage, the natural frequencies were analyzed in a little bit different way than in the first stage. They were evaluated from the frequency spectra of the measured response in each point. The response was measured only in four points on the structure therefore the mode shapes could not be determined reliably. The identified natural frequencies are shown in table 3. The obtained natural frequencies were compared with the corresponding measured ones evaluated in the course of the first stage of the experiment (see table 3). As can be seen from table 3, the frequencies measured in the 2$^{nd}$ stage were a little bit lower than in the 1$^{st}$ stage.

To fulfill the basic objective of the second stage of the experiment, the vertical acceleration measured by the standard equipment was converted to the vertical displacement using double integration in the time domain by application of Simpson's rule. However, this procedure could only evaluate the dynamic component of vertical displacement corresponding to frequencies higher than roughly 0.7 Hz.

The vertical accelerations observed in three observed points of the bridge main span during the passage of the vehicle (the van, see figure 17) in the direction from Mělice to Valy and in the opposite direction were processed in the above mentioned way. The evaluated dynamic components of the vertical displacement are shown in figure 22, the maximal peak values were 0.12 mm (in the first quarter of the main span, point No. 121), 0.07 mm (in the middle of the main span, point No. 141) and

0.11 mm (in the third quarter of the main span, point No. 161). They correspond to the displacements drawn in figure 19 that were measured by the radars. However, these results include the quasi static components beside the dynamic ones and it complicate their mutual comparison with the ones drawn in figure 22.

On the other hand, the dynamic component of the bridge response to dynamical forces induced by the group of walking pedestrians is dominant compared to the quasi static one. The mutual comparison of the results shown in figure 20 (the data measured by the radars) and figure 23 (the data measured by classic approach) is meaningful. The maximal peak values of dynamic component of the vertical displacement on figure 23 were 0.81 mm (in the first quarter of the main span, point No. 121), 1.55 mm (in the middle of the main span, point No. 141) and 0.90 mm (in the third quarter of the main span, point No. 161).

The dynamic effect of the pedestrian group that is captured in figure 23 can be also characterized by the peak value of vertical acceleration 0.31 $m \cdot s^{-2}$ (in the middle of the main span, point No. 141). The corresponding RMS value of acceleration is 0.21 $m \cdot s^{-2}$.

**Table 3.** Natural frequencies of the observed bridge evaluated during the second stage of the experiment from data obtained by the classical approach and the radar interferometry and their comparison with the corresponding ones from the first stage.

| No. (j) | Measured f(j) 2nd stage using classical approaches [Hz] | Measured f(j) 2nd stage using radar R1 and radar R2 [Hz] | Corresponding measured f(j) 1st stage [Hz] | Difference between frequencies from 2nd and 1st stage [Hz] | Character of the corresponding natural mode |
|---|---|---|---|---|---|
| **(1)** | 1.61 ± 0.02[a] | 1.62 and 1.60 | 1.62 ± 0.02[a] | -0.01 ± 0.03[a] | 1st vertical bending mode of vibration |
| **(2)** | 1.87 ± 0.02 | x | 1.89 ± 0.02 | -0.02 ± 0.03 | 1st horizontal mode of vibration of arch |
| **(3)** | 2.23 ± 0.02 | 2.22 and 2.22 | 2.25 ± 0.02 | -0.02 ± 0.03 | 2nd vertical bending mode of vibration |
| **(4)** | 2.47 ± 0.02 | x | 2.55 ± 0.02 | -0.08 ± 0.03 | 1st torsional mode of vibration |
| **(5)** | x | 3.02 and 3.02 | 3.02 ± 0.03 | 0.00 ± 0.04 | 2nd torsional mode of vibration |
| **(6)** | x | x | 3.06 ± 0.03 | x | 3rd vertical bending mode of vibration |
| **(7)** | x | 3.44 and 3.42 | 3.47 ± 0.02 | -0.04 ± 0.04 | 4th vertical bending mode of vibration |

[a] Expanded uncertainty $U_{k=2}$, x – the frequency was not reliably evaluated.

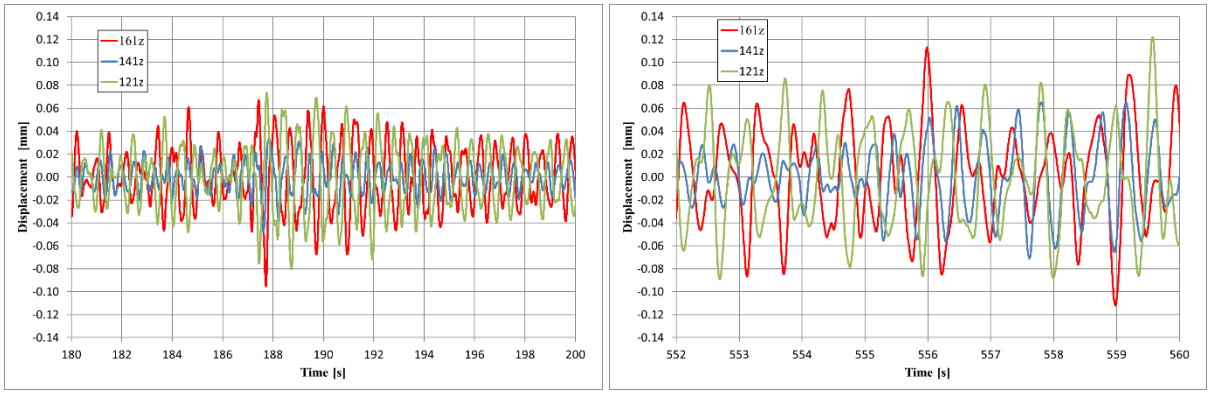


**Figure 22.** The dynamic component of vertical displacement evaluated from the measured acceleration by standard measuring equipment in first quarter (the point No. 121), in the middle (the point No. 141) and in third quarter (the point No. 161) of the bridge main span during the passage of the vehicle (the van) in the direction from Mělice to Valy (left) and in the opposite direction (right).

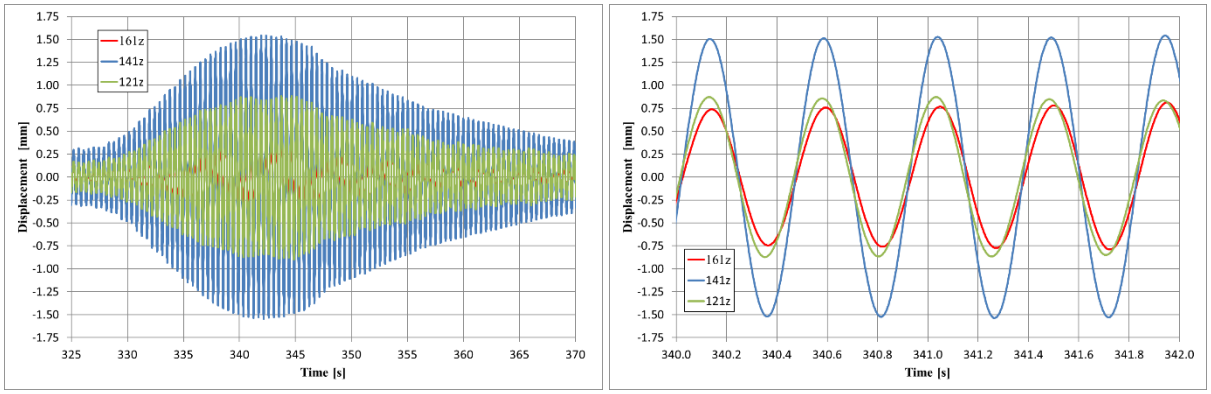


**Figure 23.** The dynamic component of vertical displacement evaluated from the measured acceleration by standard measuring equipment in first quarter (the point No. 121), in the middle (the point No. 141) and in third quarter (the point No. 161) of the bridge main span that was produced by the dynamic effect of the pedestrian group.

## 5. The third stage of the experiment

The third stage of the experiment was realized on 23rd April 2021 just by classical approach and was performed only in a substantially simplified form compared to the first stage. The first objective of this stage was to determine the fundamental natural frequencies of the bridge roughly one-year after it was put in operation. The second one was to observe and evaluate the level of forced vibration caused by the standard road traffic and pedestrians.

Based on the knowledge obtained by the first stage of the experiment, the scope of the third experiment stage was reduced and it was focused in particular on the main bridge span (the 3rd one) because this section of the bridge was the most dynamically sensitive.

### *5.1. Used standard measuring equipment and measurement system*

The standard measuring equipment used in the course of the third stage was similar to the one applied in the first and second stage.

Similar to the second stage, the standard road traffic was not limited again in the course of the third experiment stage as can be deduced from the objectives of the stage. Again, the bridge vibrations were induced both by vehicle passages over the bridge deck and by movement of pedestrian groups over sidewalks.

The AVT method was applied for results evaluation again. Two reference responses were used during realization of the third stage of the experiment. The first one was orientated in vertical direction and the second one in the horizontal direction perpendicular to the longitudinal axis of the bridge. Both reference accelerometers were placed in the first quarter of the main span (the point No. 121 according the numbering used by the first experiment stage). The bridge vibrations were recorded on the left arch in 2 selected points and 13 points were observed on the left main girder. One was placed in the middle of the second span of the bridge (the point No. 71), eleven ones were positioned in the third main span (the points No. 91, 101, 111, 121, 131, 141, 151, 161, 171, 181 and 191) and the last one was placed in the middle of the fourth span (the point No. 211).

### *5.2. Results of the third stage of the dynamic analysis*

The natural frequencies were analyzed based on CMIF again. The identified fundamental natural frequencies are shown in table 4 and selected corresponding mode shapes in figure 24 and figure 25. Two natural frequencies, that are in table 4 marked by letter “x”, could not be reliably evaluated. The

obtained natural frequencies were compared with the corresponding measured ones that were evaluated in the course of the first stage of the experiment (see table 4). As can be seen from table 4, only two natural frequencies changed recognizably. Both the 4th and the 8th frequency correspond to the torsional mode of vibration (see figure 9 for example). The probable reason for the decrease in these two frequencies was that the bridge was not entirely completed when the first stage was realized. The mass belonging to horizontal grates on the side walkways was missing on the load bearing structure because the grates were not mounted on the side cantilevers in time of the first stage of the experiment.

**Table 4.** Natural frequencies of the observed bridge evaluated during the third stage of the experiment and their comparison with the corresponding ones from the first stage.

| No. (j) | Measured f(j) 3rd stage [Hz] | Corresponding measured f(j) 1st stage [Hz] | Difference between frequencies [Hz] | Character of the natural mode |
|---|---|---|---|---|
| **(1)** | 1.62 ± 0.02[a] | 1.62 ± 0.02[a] | 0.00 ± 0.03[a] | 1st vertical bending mode of vibration |
| **(2)** | 1.89 ± 0.02 | 1.89 ± 0.02 | 0.00 ± 0.03 | 1st horizontal mode of vibration of arch |
| **(3)** | 2.24 ± 0.02 | 2.25 ± 0.02 | -0.01 ± 0.03 | 2nd vertical bending mode of vibration |
| **(4)** | 2.51 ± 0.02 | 2.55 ± 0.02 | -0.04 ± 0.03 | 1st torsional mode of vibration |
| **(5)** | x | 3.02 ± 0.03 | x | 2nd torsional mode of vibration |
| **(6)** | 3.04 ± 0.03 | 3.06 ± 0.03 | -0.02 ± 0.04 | 3rd vertical bending mode of vibration |
| **(7)** | 3.47 ± 0.02 | 3.47 ± 0.02 | 0.00 ± 0.03 | 4th vertical bending mode of vibration |
| **(8)** | 3.80 ± 0.02 | 3.84 ± 0.02 | -0.04 ± 0.03 | 3rd torsional mode of vibration |
| **(9)** | 4.00 ± 0.02 | 4.00 ± 0.02 | 0.00 ± 0.03 | 5th vertical bending mode of vibration |
| **(10)** | x | 4.73 ± 0.02 | x | 4th torsional mode of vibration |

[a] Expanded uncertainty $U_{k=2}$, x – the frequency was not reliably evaluated.

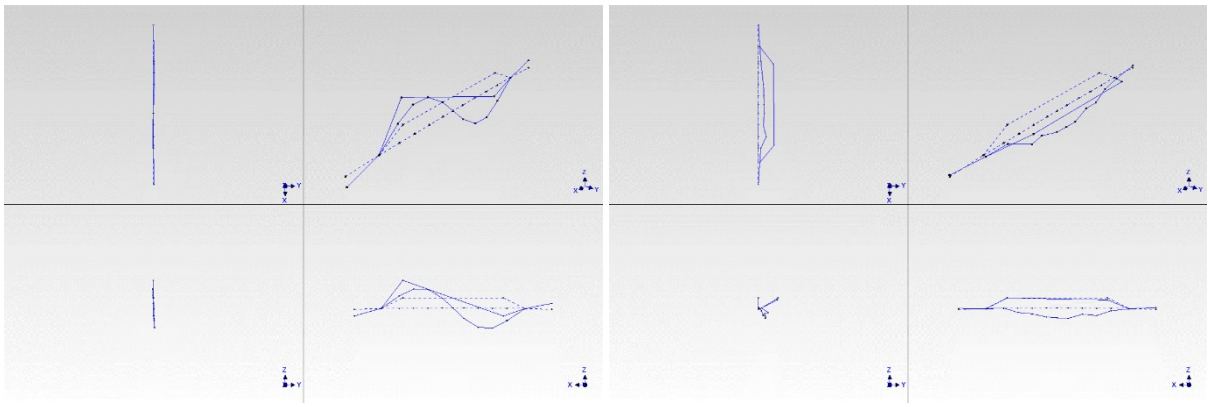

**Figure 24.** The measured 1st (on left) and 2nd (on right) natural modes of vibration evaluated from the experimental data recorded in the course of the third experiment stage.

The level of the bridge deck vibrations when the dynamic effects of the standard road traffic were observed was relatively low. The maximal peak value of vertical acceleration 0.24 $m \cdot s^{-2}$ was recorded in the middle of the bridge main span (in point No. 141) during the passage of a truck crane. Corresponding RMS value of acceleration was then 0.09 $m \cdot s^{-2}$.

The results of the third stage of the experiment again showed that the horizontal load bearing structure of the bridge is more sensitive to the dynamic effects of walking pedestrians than the ones of the road traffic. The maximal peak value of vertical acceleration 0.31 $m \cdot s^{-2}$ was recorded in the middle of the bridge main span (in point No. 141) during the passage of two pedestrians walking

synchronously with the pace frequency close to the third natural frequency of the bridge. Corresponding RMS value of acceleration was then 0.20 $m \cdot s^{-2}$.

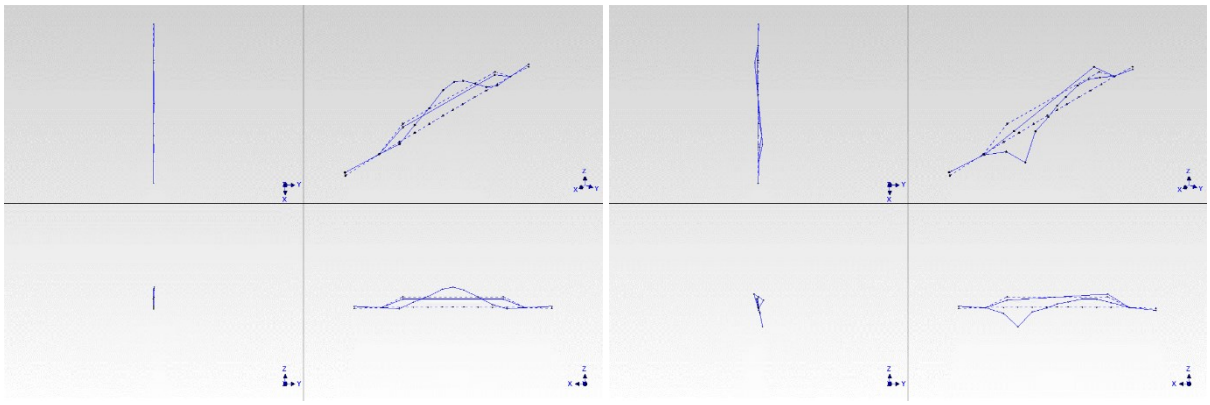

**Figure 25.** The measured 3rd (on left) and 4th (on right) natural modes of vibration evaluated from the experimental data recorded in the course of the third experiment stage.

## 6. Results and their discussion

The variants of the measurement system used in the course of the second and third stage of the experiment are limited for the detailed identification of the character of the natural modes corresponding to the investigated natural frequencies. It means, that the results of the first stage are significant also for second and third one because the shapes of the natural modes were identified in details and it is important for the correct assignation of the theoretical and experimental natural frequencies. However, the traffic on the bridge has to be restricted during the detailed investigation of the mode shapes and it means complications for such experiments carried on existing bridges.

However, when the modes are already identified in detail, the measurement systems utilized during the second and third stages are applicable for controlling the changes of the natural frequencies which may mean an undesirable change in the structural condition of the bridge load bearing structure. The results of the second and third stage of the experiments that are summarized in table 3 and table 4 showed that it is difficult to identified some natural frequencies, especially the ones corresponding to the torsional mode shapes, due to the simplified experiment arrangements.

The evaluated damping of the bridge structure is relatively small, especially for the first and third natural frequency. However, this fact does not influence negatively the level of usual bridge vibrations caused both the passing road traffic and walking pedestrians.

The dynamic responses of the bridge horizontal load bearing structure in the displacement scale to the dynamic effects of the pedestrian group that were evaluated from data measured synchronously by the radar interferometry (see figure20) and by the standard measuring equipment (see figure 23) are substantially similar. The differences between the dynamic components of vertical displacement obtained by the radar interferometry and by classical approach are much small.

## 7. Conclusions

The experiment described in this paper was realized in three stages. Each one had its own purpose. The results of all three experiment stages could be summarized to the following conclusions.

The load bearing structure of the observed bridge that is designed for standard road traffic is unusually sensitive to the dynamic effects produced by the pedestrians. In particular, the main span of the bridge can noticeably vibrate when the pace frequency of walking pedestrians is close to the third

natural frequency. However, the level of the evaluated bridge vibrations induced by the standard pedestrian traffic did not exceed the comfort limits defined in Czech standards.

The differences between the measured and corresponding theoretical natural frequencies of the load bearing structure of the investigated bridge (see table 1) were very low during the first stage of the experiment. The strictest limit deviation according to Czech standard No. 736209 is valid for the first natural frequency $f_{(1)}$ and it is +10 % and -15 % respectively. All compared pairs of the frequencies (see table 1) fulfilled standard limits with large reserve. The theoretical model of the bridge used for its design and theoretical analysis was accurate enough. The evaluated natural frequencies could be also used for further identification of the model to achieve better conformity between measured and theoretical ones.

In the time period between May 2020 and April 2021, the natural frequencies of the bridge did not change practically (see table 3 and table 4). Only two of them, the 4$^{th}$ and the 8$^{th}$ frequency, varied recognizably as can be seen, for example, from table 4. However, both these frequencies correspond to the torsional modes of vibration. The probable reason for the decrease in these two frequencies was that the bridge was not entirely completed when the first stage was realized. The horizontal grates on the walkways were not mounted on the side cantilevers. Their additionally added mass influenced likely the noticeable decrease of the natural frequencies corresponding to the torsional modes of vibration.

**Acknowledgment**
The results presented in this paper are outputs of the research project VI20192022167 “The Advanced Technology of Rapid Determination of Bridges Deformation by Radar Interferometry and its Use in Diagnostics” supported by Ministry of the Interior of the Czech Republic.

**References**

[1] M. Polak, T. Plachy, A. Citek, K Berkova, P. Hajkova, and M. Cap, “Experimental dynamic analysis of the existing footbridge in Dobřichovice town,” *MATEC Web of Conferences,* vol. 313, art. num. 00002, p. 13, 2020.
[2] J. Kasparek, P. Ryjacek, T. Rotter, M. Polak, and R. Calcada, “Long-term monitoring of the track-bridge interaction on an extremely skew steel arch bridge,“ *J. Civil. Struct. Health. Monit.*, vol. 10, pp. 377–387, 2020.
[3] P. Ryjacek, M. Polak, T. Plachy, J. Kašparek, “The dynamic behavior of the extremely skew railway bridge "Oskar"," *Procedia Structural Integrity*, vol. 5, pp. 1051-1056, 2017.
[4] M. Polak, T. Plachy, and P. Ryjacek, “Experimental dynamic analysis of the railway bridge near Zatec,” *EAN 2020 58th International Scientific Conference on Experimental Stress Analysis*, pp. 417–422, 2020.
[5] T. Plachý, M. Polák, and P. Ryjáček, “Assessment of an Old Steel Railway Bridge Using Dynamic Tests,” *Procedia Engineer.*, vol. 199, pp. 3053 – 3058, 2017.
[6] M. Talich, “The Effect of Temperature Changes on Vertical Deflections of Metal Rail Bridge Constructions Determined by the Ground Based Radar Interferometry Method,” *IOP Conference Series: Earth and Environmental Science*, vol. 221(1), 2019.
[7] M. Talich, “Using Ground Radar Interferometry for Precise Determining of Deformation and Vertical Deflection of Structures,” *IOP Conference Series: Earth and Environmental Science*, vol. 95(3), 2017.
[8] M. Sokol and K. Lamperova,” Dynamic response of bridges tested by radar interferometry,” *Vibroengineering Procedia*, vol. 23, pp. 138 – 143, 2019.
[9] C. Gentile, “Dynamic investigation of a suspension footbridge using accelerometers and microwave interferometer,” *MATEC Web of Conferences*, vol. 24, 2015.
[10] I. Lipták, J. Erdélyi, P. Kyrinovič, A. Kopáčik, "Monitoring of Bridge Dynamics by Radar

Interferometry", *INGEO 2014, 6th International Conference on Engineering Surveying*, pp. 211-216, 2014.

[11] X. Liu, X. Tong, K. Ding, X. Zhao, L. Zhu and X. Zhang, "Measurement of Long-Term Periodic and Dynamic Deflection of the Long-Span Railway Bridge Using Microwave Interferometry," *IEEE Journal of Selected Topics in Applied Earth Observations and Remote Sensing*, vol. 8, no. 9, pp. 4531-4538, 2015.

[12] R.J. Allemang, Brown D.L., "A Complete Review of the Complex Mode Indicator Function (CMIF) with Applications" *Proceedings of the Int. Conf. on Noise and Vibration Engineering (ISMA), Katholieke Universiteit Leuven, Belgium*, 38 pp., 2006.

[13] P. Avitabile, "Modal space - in our own little world", *Experimental Techniques* 37, 2, pp. 3–5, 2015.

[14] A. V. Oppenheim, R. W. Schafer, J. R. Buck, "Discrete-time signal processing" (2nd ed.), Upper Saddle River, N.J.: Prentice Hall, 1999.